BMB
Reports

BMB Rep. 2024; 57(6): 299-304
www.bmbreports.org

Tumor antigen PRAME is a potential therapeutic target of p53 activation in melanoma cells

Yong-Kyu Lee[1,#], Hyeon Ho Heo[1,#], Nackhyoung Kim[1], Ui-Hyun Park[1], Hyesook Youn[1], Eun-Yi Moon[1], Eun-Joo Kim[2] & Soo-Jong Um[1,]*

[1]Department of Integrative Bioscience and Biotechnology, Sejong University, Seoul 05006, [2]Department of Molecular Biology, Dankook University, Cheonan 31116, Korea

Upregulation of *PRAME* (preferentially expressed antigen of melanoma) has been implicated in the progression of a variety of cancers, including melanoma. The tumor suppressor p53 is a transcriptional regulator that mediates cell cycle arrest and apoptosis in response to stress signals. Here, we report that *PRAME* is a novel repressive target of p53. This was supported by analysis of melanoma cell lines carrying wild-type p53 and human melanoma databases. mRNA expression of *PRAME* was downregulated by p53 overexpression and activation using DNA-damaging agents, but upregulated by p53 depletion. We identified a p53-responsive element (p53RE) in the promoter region of *PRAME*. Luciferase and ChIP assays showed that p53 represses the transcriptional activity of the *PRAME* promoter and is recruited to the p53RE together with HDAC1 upon etoposide treatment. The functional significance of p53 activation-mediated *PRAME* downregulation was demonstrated by measuring colony formation and p27 expression in melanoma cells. These data suggest that p53 activation, which leads to *PRAME* downregulation, could be a therapeutic strategy in melanoma cells. [BMB Reports 2024; 57(6): 299-304]

INTRODUCTION

Preferentially expressed antigen in melanoma (PRAME) was discovered as a melanoma-associated antigen recognized by cytotoxic T lymphocytes (CTL) (1). Like other cancer-testis antigens (CTAs), PRAME is not detected in normal tissues except germline tissues but is highly expressed in tumors of several histological types (2, 3). Elevated *PRAME* expression is associated with poor outcomes in neuroblastoma and breast cancer (4, 5). Recent immunohistochemical analysis revealed an increased expression of PRAME in primary and metastatic melanoma compared to normal nevi (6-8). The tumor promoting activity of PRAME was discovered via its depletion in xenograft mouse tumor models (9-11). Therefore, targeting PRAME, either by exploiting its immunogenic or oncogenic potential, has been proposed as a strategy for tumor therapy (12, 13). *PRAME* expression is upregulated by promoter DNA hypomethylation (14, 15) and is stimulated by cooperation with myeloid zinc finger 1 (16). However, little is known about how *PRAME* expression is downregulated in response to anti-tumor signaling.

Tumor suppressor protein p53, encoded by *TP53*, has been a focus of cancer research. Many stress signals, in particular DNA damage, promote p53 activation and stabilization via posttranslational modifications (PTMs), such as phosphorylation and acetylation (17). Acetylation of p53 is mediated by acetyltransferases including CBP/p300, and is counteracted by histone deacetylases (HDACs) and SIRT1 (18). As a nuclear transcription factor, p53 binds to the p53 response element (p53RE) comprising two 5′-RRRCWWGYYY-3′ decamers separated by a spacer of 0-13 base pairs (R = A/G, W = A/T, Y = C/T), and regulates the expression of a variety of target genes involved in cell cycle arrest, apoptosis, DNA repair, and senescence (19). Compared to the transactivation, p53-dependent transcriptional repression has proposed mechanisms: indirectly by p21 induction followed by activation of the DREAM repressive complex, or by binding directly to the target gene promoter (20, 21).

The opposite functions of tumor antigen PRAME and tumor suppressor p53 prompted us to investigate the role of p53 in the expression of *PRAME*. The PRAME level is downregulated in inverse proportion to p53 expression in melanoma cell lines. Here, we report the mechanism underlying p53-mediated PRAME repression in response to DNA damage. Because *TP53* is rarely mutated in melanoma compared to a rate of ~50% in other tumors, p53-activating agents may have therapeutic potential for melanoma via transcriptional repression of *PRAME*.

*Corresponding author. Tel: +82-2-3408-3641; Fax: +82-2-3408-4334; E-mail: umsj@sejong.ac.kr
#These authors contributed equally to this work.

https://doi.org/10.5483/BMBRep.2023-0246

Received 26 December 2023, Revised 12 March 2024, Accepted 23 April 2024, Published online 25 April 2024

Keywords: Melanoma, p53 activation, PRAME, Repression, Transcription

ISSN: 1976-670X (electronic edition)

RESULTS

Inverse correlation between PRAME and p53 expression

To investigate the relationship between PRAME and p53, we evaluated protein levels in 15 cancer cell lines (Supplementary Table 1). In five melanoma cell lines, the PRAME protein levels are proportional to the metastatic and proliferative potentials of melanoma cells (16), and negatively correlated with p53 expression (Fig. 1A, *top*). Similar increases in *PRAME* mRNA levels were detected by RT-PCR (Fig. 1A, *bottom*). There was an inverse correlation between PRAME and p53 (R^2 = 0.9351) (Fig. 1B). A similar correlation was observed in the other eight cell lines, albeit with smaller R^2 values (Supplementary Fig. 1). Using the GSE4570 human dataset, we observed that the *PRAME* mRNA level is significantly increased in melanoma compared to normal samples (Fig. 1C), whereas *p53* expression was increased in normal melanocyte compared with melanoma samples (Fig. 1D). Further assessment of the Pearson correlation coefficient in the GSE4570 dataset yielded an adjusted R^2 value of 0.4626, suggesting a significant inverse correlation of *p53* and *PRAME* expression in human melanoma (Fig. 1E).

p53 activation causes *PRAME* downregulation

To determine whether *PRAME* expression is regulated by p53, we first overexpressed *p53* in HCT116 ($p53^{-/-}$) and *p53*-null H1299 cells, and then measured the expression level of PRAME. As shown in Fig. 2A, PRAME protein expression in both cell lines was downregulated by *p53* overexpression. In contrast, PRAME protein and mRNA levels was upregulated by depleting *p53*, accompanied with downregulation of p27, a negative target of PRAME (Fig. 2B) (16). To determine the effect of p53 activation on *PRAME* expression, A375P melanoma cells were treated with etoposide (ETO), a p53-inducing DNA-damaging agent. As shown in Fig. 2C, the protein and mRNA levels of *PRAME* decreased with increasing duration of ETO treatment. Likewise, ultraviolet C (UV-C) and methyl methane sulfonate (MMS) reduced the PRAME level in A375P cells (Fig. 2D). PRAME was also downregulated in the A375SM and TXM-13 melanoma cell lines upon ETO-induced p53 activation, as determined by visualizing acetylated p53 (Supplementary Fig. 2A). Also, similar assays were performed using *p53*wt and $p53^{-/-}$ HCT116 cells under two genotoxic conditions. Compared to *p53*wt HCT116 cells, no significant suppression of PRAME expression was observed in *p53*-null HCT116 cells,

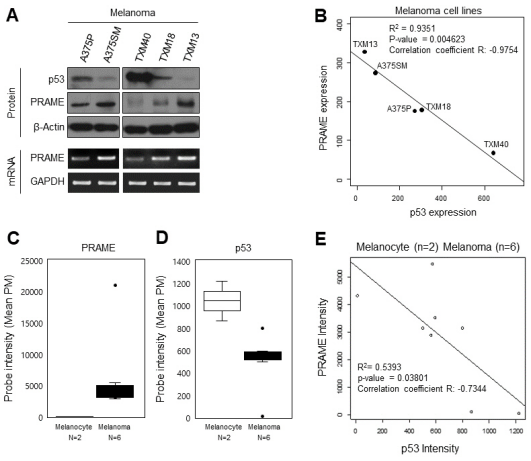

Fig. 1. Negative correlation between PRAME and p53. (A) Negative correlation between p53 and PRAME expression in melanoma cell lines. Protein and mRNA levels were measured by Western blot and RT-PCR, respectively (n = 1). (B) Correlation coefficient between p53 and PRAME. The band densities of p53 and PRAME in Fig. 1A were quantified utilizing ImageJ software. (C, D) Comparison of p53 and PRAME expression. Using the GSE4570 data set, mRNA levels of p53 and PRAME were assessed in normal melanocytes (n = 2) and melanoma (n = 6). (E) Correlation of p53 and PRAME mRNA levels assessed by calculating the Pearson correlation coefficient using the GSE4570 data set. All Pearson correlation tests and linear regression analyses were performed using MedCalc software.

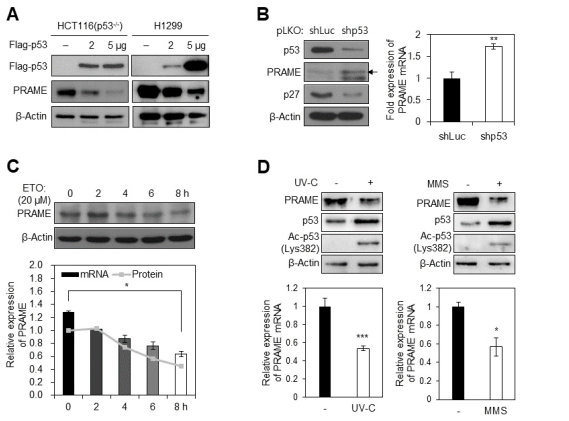

Fig. 2. Downregulation of PRAME by p53 activation. PRAME mRNA expression was assessed via RT-qPCR, and the data were displayed as means ± SD (n = 3, *P < 0.05; **P < 0.01; ***P < 0.005). Proteins were visualized by WB using indicated antibodies (n = 1). (A) Negative effect of p53 on PRAME expression. PRAME protein was visualized by WB in HCT116$p53^{-/-}$ and p53-null H1299 cells transfected with Flag-p53 expression vector (2 and 5 μg) (n = 3). (B) Effect of p53 knockdown on PRAME expression. HCT116 cells carrying wild-type p53 were transfected with a luciferase control or p53 shRNA. Twenty-four hours after transfection, the protein levels of PRAME and p27 were measured by WB (n = 1). PRAME mRNA expression was measured by RT-qPCR (n = 3, **P < 0.01). (C) Effect of ETO on PRAME expression. A375P cells were treated with 20 μM etoposide (ETO) for indicated times. Proteins were visualized by WB. PRAME band intensity was measured by ImageJ software and normalized to β-actin. The PRAME mRNA level was quantified by RT-qPCR and normalized to GAPDH (n = 3, *P < 0.05). (D) Effects of UV-C and MMS on PRAME expression. A375P cells were treated with 50 J/m^2 UV-C or 2 mM methyl methane sulfonate (MMS). Proteins were visualized by WB using indicated antibodies (n = 3). PRAME mRNA levels were quantified using RT-qPCR and normalized to GAPDH (n = 3, *P < 0.05; ***P < 0.005).

suggesting that *PRAME* repression by p53 activation is p53-dependent (Supplementary Fig. 2B). The response to MMS was less p53-dependent (data not shown). Together, these data suggest that *PRAME* expression is negatively regulated by p53 activation in melanoma cells.

p53 binds to the *PRAME* promoter and recruits HDAC1

To investigate the mechanism by which p53 represses *PRAME* expression, we isolated a regulatory sequence of the human *PRAME* gene and subcloned it into the pGL2 basic luciferase reporter vector. *In silico* analysis revealed two putative p53 response elements (upstream RE1, −1835/−1808, and downstream RE2, +1511/+1543) at −3556 to +2444 of *PRAME* promoter (Supplementary Fig. 3A). HCT116*p53*wt and HCT-116*p53*$^{-/-}$ cells were transfected with a luciferase reporter containing the −3556/+2444 region of the *PRAME* gene and the Flag-p53 vector. Luciferase assays indicated that the transcriptional activity of *PRAME* was significantly downregulated by *p53* overexpression in both cell lines (Supplementary Fig. 3B). To identify the RE responsible for p53-dependent transcriptional repression, various truncation mutants were constructed and transfected with the Flag-p53 expression vector (Fig. 3A). Constructs containing −2667/+2444 and −1864/+2444 were transcriptionally repressed by p53, whereas other deletions lacking upstream RE1 did not respond to ectopically expressed p53 (Fig. 3B). Four additional mutants were generated in the promoter region of *PRAME*: mutRE, base substitution; ΔRE1 (RE1 deletion), −1806/+2444; −2667/+1, RE1-positive; −1778/+1, RE1-negative (Fig. 3C and Supplementary 3C). Compared to wild-type, mutRE and ΔRE1 were not repressed by p53 (Fig. 3D). No p53-mediated repression was observed upon deletion of RE1 (−1778/+1) (Supplementary 3C). Overall, these data suggest that the p53RE1 upstream of *PRAME* is responsible for p53-mediated repression.

To determine whether p53 binds to RE1 or RE2 of *PRAME*, we performed chromatin immunoprecipitation (ChIP) using primer sets covering RE1 and RE2 of *PRAME*, and p53RE of *p21* as the positive control. Like the p53RE of *p21*, the p53RE1 of *PRAME* was occupied by Flag-tagged p53 (Supplementary 3D), which was verified by quantitative PCR following ChIP (Fig. 3E). Further, ETO treatment increased the occupancy of endogenous p53 in the RE1 of *PRAME* in A375P cells (Supplementary 3E). Subsequent quantification revealed that the enrichment of p53 and HDAC1 at p53RE1 is significantly enhanced in response to ETO treatment (Fig. 3F). As expected, the level of acetylated histone H3 at lysine 9 (H3K9ac), a substrate of HDAC1, was downregulated (Fig. 3F). These findings suggest that p53 represses the transcriptional expression of *PRAME* by binding p53RE1 in the *PRAME* promoter and recruiting HDAC1, leading to downregulation of H3K9ac, an active histone code.

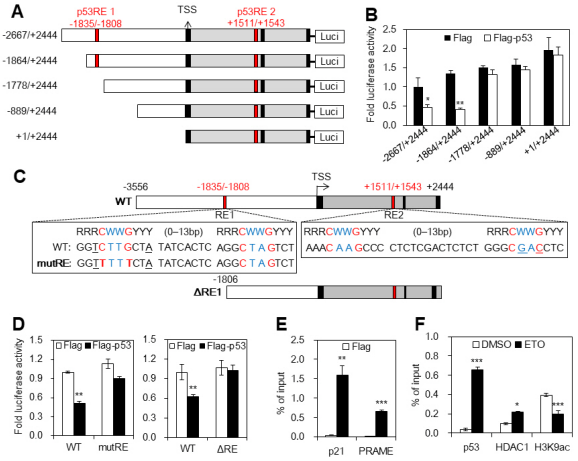

Fig. 3. p53 binds to the *PRAME* promoter and recruits HDAC1. (A, B) Mapping of functional p53RE. Five deletion constructs carrying the luciferase gene (A) were introduced into HCT116*p53*$^{-/-}$ cells with the Flag-p53 vector for luciferase assays (B). Luciferase data are means ± SD (n = 3). *P < 0.05; **P < 0.01. (C) Nucleotide sequences of p53RE1 and RE2. Two mutants are displayed: mutRE, base substitution; ΔRE1, RE1 deletion. (D) Effect of RE1 mutation on p53-dependent transcriptional repression of the PRAME promoter. HCT116p53$^{-/-}$ cells were transfected with mutRE (left), ΔRE1 (right) with the Flag-p53 vector. Cell lysates were subjected to luciferase assays. Luciferase data are means ± SD (n = 3). **P < 0.01. (E) p53 binding to the RE1 of the *PRAME* promoter. H1299 cells were transfected with Flag or Flag-p53 for ChIP using an anti-Flag antibody. qPCR was performed using primer sets covering p53RE1 and RE2 of *PRAME*. The p53RE in *p21* was used as the positive control. Quantification of ChIP-qPCR data; means ± SD (n = 3). **P < 0.01; ***P < 0.005. (F) HDAC1 recruitment to the RE1 of the *PRAME* promoter. A375 cells were treated with ETO and subjected to ChIP assay using antibodies against p53, histone deacetylase 1 (HDAC1), and acetylated histone H3 at lysine 9 (H3K9ac). Quantification was performed by qPCR using a primer set covering the RE1 of *PRAME*. Data are means ± SD (n = 3). *P < 0.05; ***P < 0.005.

PRAME loss mimics ETO treatment in proliferation of melanoma cells and p27 induction

As described previously, *PRAME* increases the proliferation of melanoma cells (16). To determine whether p53-dependent *PRAME* repression occurs at the cellular level, we evaluated the effect of *PRAME* knockdown and ETO treatment on the proliferation of melanoma cells. Colony formation was significantly decreased by *PRAME* depletion (Fig. 4A, B, *left*) and ETO treatment (Fig. 4A, B, *right*) in A375P and A375SM cells. Colony formation by *p53*-high/*PRAME*-low A375P cells was less efficient than by *p53*-low/*PRAME*-high A375SM cells. Other effects of PRAME loss and ETO treatment were investigated by monitoring expression of the cell cycle inhibitor p27 (also known as KIP1). As shown in Fig. 4C, the protein levels of p53 and PRAME were opposite in A375P and A375SM cells. p27 was upregulated by *PRAME* knockdown and ETO treatment in A375P cells. Taken together, these results suggest that ETO-

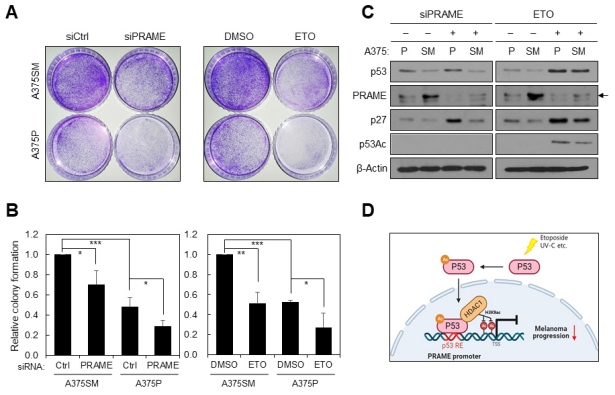

Fig. 4. *PRAME* knockdown and ETO treatment suppress melanoma cell proliferation and p27 induction. (A) Effects of *PRAME* depletion and ETO treatment. A375SM or A375P cells were transfected with siPRAME (left) or treated with 20 μM ETO (right) and subjected to colony formation assay (n = 3). Control siRNA (siCtrl) is an unspecific scrambled siRNA purchased from Bioneer (Korea). Colonies were fixed and stained with crystal violet. (B) The number of colonies was counted from three independent experiments and the relative numbers are shown. Data are mean ± SD (n = 3). *P < 0.05; **P < 0.01; ***P < 0.005. (C) Upregulation of p27 by *PRAME* depletion and ETO treatment. Cell lysates prepared as described above were subjected to WB using the indicated antibodies (n = 1). β-Actin was used as the internal control. (D) Hypothetical model for the p53-mediated PRAME downregulation through HDAC1 recruitment.

induced p53 activation suppresses the proliferation of melanoma cells through the downregulation of *PRAME*.

DISCUSSION

High *PRAME* expression has been implicated in the progression of several tumors, including melanoma. However, no attempts have been made as yet to control the *PRAME* expression. Here we present evidence that p53 activation exerts transcriptional repression of *PRAME*: increased PRAME expression and downregulation upon p53 knockdown and overexpression, respectively; higher luciferase activity of the PRAME-luciferase reporter gene in *p53*-null cells than in *p53*wt cells. In addition, we demonstrated that *PRAME* repression by p53 activation is p53-dependent. Finally, we dissected the underlying mechanism and suggested that p53 binds to the p53 response element in the *PRAME* promoter and recruits histone deacetylase 1, leading to the reduced accumulation of acetylated histone H3 at lysine 9 (Fig. 4D). Our findings support that *PRAME* may be a potential therapeutic target of p53 activation in melanoma.

The mutation frequency of *p53* in melanoma is 10-20%, compared to about 50% in other tumors (22, 23). Intriguingly, p53 is frequently inactivated in melanoma harboring wild-type p53 (24, 25). Given the 10-20% mutation rate of *p53* in melanoma, the next question is raised whether the PRAME mRNA expression is higher in *p53*-mutant melanoma samples. From the analysis of the TCGA human melanoma databases using the UALCAN and USCS Xena browser tools, we did not see a statistically significant difference in *PRAME* expression between patients carrying *p53*wt and mutant *p53*. This observation may be due to the small population of patients with a particular p53 mutation because of the low mutation rate of *p53* in melanoma and the variety of *p53* mutations, including nonsense, missense, deletion, and frameshift mutations. At present, it is not clear whether *p53* mutations result in *p53* loss or point mutations. It is well established that hotspot forms of *p53* mutations, mostly accumulated in the DNA binding domain (DBD), alter the transcription of target genes and become oncogenic (26). For example, p53 DBD mutants (R273H, R175H) enhance the transcriptional activity of *CXCL5* and *CXCL8* (27), while suppressing the expression of the differentiation inhibitor Id2 (28) and the apoptosis receptor CD95 (29). Like *Id2* and *CD95*, mutant p53 may inhibit *PRAME* expression. However, it is more plausible that mutant p53 does not affect *PRAME* repression or instead increases *PRAME* expression in cancer cells that require the oncogenic properties of PRAME. Further studies are needed to determine whether mutant p53, such as mutants in the DNA binding domain or transactivation domain, represses *PRAME* expression.

MATERIALS AND METHODS

RNA interference

To deplete PRAME mRNA, we used siPRAME targeting exon 3 (sense strand, 5′-CAGUAGAGGUGCUCGUAGA (dTdT)-3′; antisense strand, 5′-UCUACGAGCACCUCUACUG (dTdT)-3′) (Bioneer, Korea). siRNA transfection was performed with Lipofectamine RNAiMAX (Invitrogen) according to the manufacturer's instructions. Non-targeting scramble siRNA was also purchased from Bioneer (SN-1001) and used as a negative control. For p53 knockdown, shp53 pLKO.1 was purchased from Addgene (Watertown, MA, USA), (sense strand, 5′-CCGACTCCAGTGGTAATC TACTTCAAGAGAGTAGATTACCACTGGAGTCTTTTT-3′; antisense strand, 5′-AAAAAGACTCCAGTGGTAATCTACTCTC TTGAAGTAGATTACCACTGGAGTCGG-3′ with the p53 target region shown in bold type). As a negative control, the sh-luciferase (shLuc) sequence, subcloned into the pLKO.1 vector, was also purchased from Addgene.

Real-time reverse transcription-quantitative PCR (RT-qPCR)

Total RNA was extracted by standard methods using Isol-RNA Lysis Reagent (5 PRIME, Germany). cDNA synthesis was performed using M-MLV reverse transcriptase and random primers (Invitrogen). Semi-quantitative PCR was conducted with G-Taq (Labopass, Korea). For quantitation, real-time PCR reactions were performed using SYBR® Green Real-time PCR Master Mix (TOYOBO, Japan) and CFX96 Real-Time PCR Detection System (Bio-Rad, CA, USA) with the following primer pairs (forward and reverse, respectively): PRAME, 5′-CGTTTGTGG GGTTCCATTC-3′ and 5′-GCTCCCTGGGCAGCAAC-3′; p21, 5′-

CTGGAGACTCTCAGGGTC-3′ and 5′-TTAGGGCTTCCTCTTG GAGA-3′; and GAPDH, 5′-GACTCCACGACGTACTCA-3′ and 5′-GTGGATATTGTTGCCATC-3′. Murine primer sets are: p53, 5′-TGCTCACCCTGGCTAAAGTT-3′ and 5′-AATGTCTCCTGG CTCAGAGG-3′; p21, 5′-TGTCGCTGTCTTGCACTCTG-3′ and 5′-CGTGGGCACTTCAGGGTTTT-3′; Pcna, 5′-GGGGTGAAGT TTTCTGCAAGT-3′ and 5′-TCAGAGCAAACGTTAGGTGAAC-3′; Prame, 5′-TCTTCTGGGGGCCCTAAGTT-3′ and 5′-GGCTG GATTGCAGACTGACT-3′. All primer sequences were verified using Primer-Blast provided by NCBI. Results were normalized to GAPDH transcript levels as an internal standard.

Western blotting (WB)

For WB, cells were lysed in RIPA buffer (50 mM Tris-Cl pH 7.5, 150 mM NaCl, 0.4% Nonidet P-40, 1 mM EDTA, 1 mM PMSF, 1 mM Na_3VO_4, and 1 mM NaF) supplemented with a protease inhibitor cocktail (Roche, Switzerland). Proteins were separated by electrophoresis on 8-15% SDS gels, transferred to nitrocellulose, and incubated with the following primary antibodies: anti-PRAME (sc-137188, Santa Cruz Biotechnology, CA, USA; ab219650, Abcam, Cambridge, UK), anti-p53 (sc-6243; Santa Cruz Biotechnology), anti-acetyl-p53 (Lys 382) (#2525; Cell Signaling Technology, MA, USA), anti-p27 (sc-528; Santa Cruz Biotechnology), and anti-β-actin (sc-47778; Santa Cruz Biotechnology). Blots were next incubated with goat anti-mouse IgG-HRP (sc-2005; Santa Cruz Biotechnology) or goat anti-rabbit IgG-HRP (sc-2004; Santa Cruz Biotechnology).

Chromatin immunoprecipitation (ChIP)

ChIP analysis was conducted as described previously (16). Cross-linked sheared chromatin complexes were recovered by IP using IgG, anti-p53 (sc-6243; Santa Cruz Biotechnology), anti-H3K9Ac (ab10812; Abcam), anti-HDAC1 (05-614; Upstate Biotechnology, NY, USA), and anti-Flag M2 (F1804; Sigma-Aldrich). The cross-linking was reversed according to Millipore's protocol. DNA pellets were recovered and analyzed by semi-quantitative PCR and RT-qPCR with the following primer pairs (forward and reverse, respectively): PRAME p53RE1, 5′-AGGAATGTCTTGCAGGGCTA-3′ and 5′-AAGGGCTCATGCT TACATGG-3′; PRAME p53RE2, 5′-CCCATCTGCTCCCCACC-3′ and 5′-CCAGGGCAAAATCTCACGA-3′, and p21 p53RE; 5′-TGGCTCTGATTGGCTTTCT-3′ and 5′-TGGGGTCTTTAGA GGTCTCC-3′.

Colony formation assay

A375P and A375SM cells were transfected with siRNA or treated with etoposide (ETO, 20 μM) for 2 days before seeding in 60 mm culture dishes at a density of 3,000 cells per dish. Ten days after plating, colony formation was monitored by crystal violet staining. Stained colonies were counted from three independent assays and relative colony counts were displayed.

Statistical analysis

Statistical analyses were conducted using SigmaPlot (version 10.0; Systat Software, USA) and MedCalc (version 22.021; MedCalc Software, Belgium). The correlation between PRAME and TP53 levels was assessed using Pearson correlation test and linear regression analysis. Student's t-test was used to compare statistical significance between groups. Data are presented as mean ± standard deviation (SD) of at least three independent experiments. Protein band density was measured using ImageJ (version 1.52e, National Institutes of Health, USA). P-values < 0.05(*), 0.01(**), or 0.005(***) were considered statistically significant.

SUPPLEMENTARY METHODS

Some additional information on Materials and Methods can be found in the supplementary section.

ACKNOWLEDGEMENTS

This study was supported by the Basic Research Program through the National Research Foundation of Korea (NRF) funded by the Ministry of Science and ICT (2021R1A4A5 033289), and also supported by Korea Basic Science Institute (National research Facilities and Equipment Center) grant funded by the Ministry of Education (2023R1A6C101A045).

CONFLICTS OF INTEREST

The authors have no conflicting interests.

REFERENCES

1. Ikeda H, Lethé B, Lehmann F et al (1997) Characterization of an antigen that is recognized on a melanoma showing partial HLA Loss by CTL expressing an NK inhibitory receptor. Immunity 2, 199-208
2. Xu Y, Zou R, Wang J, Wang ZW and Zhu X (2020) The role of the cancer testis antigen PRAME in tumorigenesis and immunotherapy in human cancer. Cell Prolif 53, e12770
3. Kern CH, Yang M and Liu WS (2021) The PRAME family of cancer testis antigens is essential for germline development and gametogenesis. Biol Reprod 105, 290-304
4. Oberthuer A, Hero B, Spitz R, Berthold F and Fischer M (2004) The tumor-associated antigen PRAME is universally expressed in high-stage neuroblastoma and associated with poor outcome. Clin Cancer Res 10, 4307-4313
5. Epping MT, Hart AA, Glas AM, Krijgsman O and Bernards R (2008) PRAME expression and clinical outcome of breast cancer. Br J Cancer 99, 398-403
6. Cazzato G, Colagrande A, Ingravallo G et al (2022) PRAME immuno-expression in cutaneous sebaceous carcinoma: a single institutional experience. J Clin Med 11, 6936
7. Cazzato G, Cascardi E, Colagrande A et al (2022) PRAME immunoexpression in 275 cutaneous melanocytic lesions: a double institutional experience. Diagnostics (Basel) 12, 2197

8. Cascardi E, Cazzato G, Ingravallo G et al (2023) PReferentially Expressed Antigen in MElanoma (PRAME): preliminary communication on a translational tool able to early detect oral malignant melanoma (OMM). J Cancer 14, 628-633
9. Yan H, Zhao RM, Wang ZJ, Zhao FR and Wang SL (2015) Knockdown of PRAME enhances adriamycin-induced apoptosis in chronic myeloid leukemia cells. Eur Rev Med Pharmacol Sci 19, 4827-4834
10. Zhu H, Wang J, Yin J et al (2018) Downregulation of PRAME suppresses proliferation and promotes apoptosis in hepatocellular carcinoma through the activation of p53 mediated pathway. Cell Physiol Biochem 45, 1121-1135
11. Chen X, Jiang M, Zhou S et al (2023) PRAME promotes cervical cancer proliferation and migration via Wnt/β-catenin pathway regulation. Cancers (Basel) 15, 1801
12. Bose M (2023) Preferentially expressed antigen in melanoma is a multifaceted cancer testis antigen with diverse roles as a biomarker and therapeutic target. Int J Transl Med 3, 334-359
13. Cassalia F, Danese A, Tudurachi I et al (2024) PRAME updated: diagnostic, prognostic, and therapeutic role in skin cancer. Int J Mol Sci 25, 1582
14. Qian J, Zhu ZH, Lin J et al (2011) Hypomethylation of PRAME promoter is associated with poor prognosis in myelodysplastic syndrome. Br J Haematol 154, 153-155
15. Zhang W, Barger CJ, Eng KH et al (2016) PRAME expression and promoter hypomethylation in epithelial ovarian cancer. Oncotarget 7, 45352-45369
16. Lee YK, Park UH, Kim EJ, Hwang JT, Jeong JC and Um SJ (2017) Tumor antigen PRAME is up-regulated by MZF1 in cooperation with DNA hypomethylation in melanoma cells. Cancer Lett 403, 144-151
17. Dai C and Gu W (2010) p53 post-translational modification: deregulated in tumorigenesis. Mol Med 16, 528-536
18. Lee JY and Gu W (2013) SIRT1: regulator of p53 deacetylation. Genes Cancer 4, 112-117
19. Riley T, Sontag E, Chen P and Levine A (2008) Transcriptional control of human p53-regulated genes. Nat Rev Mol Cell Biol 9, 402-412
20. Ceribelli M, Alcalay M, Viganò MA and Mantovani R (2006) Repression of new p53 targets revealed by ChIP on chip experiments. Cell Cycle 5, 1102-1110
21. Rinn JL and Huarte M (2011) To repress or not to repress: this is the guardian's question. Trends Cell Biol 21, 344-353
22. Luca M, Lenzi R, Leejackson D, Gutman M, Fidler I and Bareli M (1993) p53 mutations are infrequent and do not correlate with the metastatic potential of human-melanoma cells. Int J Oncol 3, 19-22
23. Weiss J, Heine M, Arden KC et al (1995) Mutation and expression of TP53 in malignant melanomas. Recent Results Cancer Res 139, 137-154
24. Houben R, Hesbacher S, Schmid CP et al (2011) High-level expression of wild-type p53 in melanoma cells is frequently associated with inactivity in p53 reporter gene assays. PLoS One 6, e22096
25. Avery-Kiejda KA, Bowden NA, Croft AJ et al (2011) p53 in human melanoma fails to regulate target genes associated with apoptosis and the cell cycle and may contribute to proliferation. BMC Cancer 11, 203
26. Pfister NT and Prives C (2017) Transcriptional regulation by wild-type and cancer-related mutant forms of p53. Cold Spring Harb Perspect Med 7, a026054
27. Yeudall WA, Vaughan CA, Miyazaki H et al (2012) Gain-of-function mutant p53 upregulates CXC chemokines and enhances cell migration. Carcinogenesis. 33, 442-451
28. Yan W, Liu G, Scoumanne A and Chen X (2008) Suppression of inhibitor of differentiation 2, a target of mutant p53, is required for gain-of-function mutations. Cancer Res 68, 6789-6796
29. Zalcenstein A, Stambolsky P, Weisz L et al (2003) Mutant p53 gain of function: repression of CD95 (Fas/APO-1) gene expression by tumor-associated p53 mutants. Oncogene 22, 5667-5676